International Journal of Current Advanced Research
ISSN: O: 2319-6475, ISSN: P: 2319-6505, Impact Factor: SJIF: 5.995
Available Online at www.journalijcar.org
Volume 6; Issue 12; December 2017; Page No. 8503-8509
DOI: http://dx.doi.org/10.24327/ijcar.2017.8509.1374

Research Article

ANIONIC FORMATION IN LOW-ENERGY ELECTRON SCATTERING FROM LARGE FULLERENES: THEIR MULTIPLE FUNCTIONALIZATION

Msezane A. Z[1]*., Felfli Z[1]., Shaginyan V. R[1,2] and Amusia M. Ya[3, 4]

[1]Department of Physics and Center for Theoretical Studies of Physical Systems, Clark Atlanta University, Atlanta, Georgia 30314, USA
[2]Petersburg Nuclear Physics Institute, NRC Kurchatov Institute, Gatchina 188300, Russian Federation
[3]Racah Institute of Physics, Hebrew University, Jerusalem 91904, Israel
[4]Ioffe PhysicalTechnical Institute, Sankt-Petersburg 194021, Russian Federation

A R T I C L E I N F O

Article History:
Received 6th September, 2017
Received in revised form 25th October, 2017
Accepted 4th November, 2017
Published online 28th December, 2017

Key words:
Large fullerenes, organic solar cells, Regge poles, anionic catalysis, electron scattering

A B S T R A C T

The first low-energy electron elastic scattering total cross sections (TCSs) for C_{94}, C_{96}, C_{98}, C_{120} and C_{136} fullerenes are reported. From the TCSs, calculated using our robust Regge pole methodology which fully embeds the crucial electron-electron correlations and the vital core-polarization interaction, we extract the binding energies (BEs) of the resultant anions formed during the collisions. Characterized by correlation and polarization induced dramatically sharp resonances manifesting long-lived metastable anionic formation, the TCSs demonstrate that when subjected to varying gentle electron impact energy the investigated fullerenes respond through rich resonance structures, representing doorway states to stable ground state anionic formation. These results significantly widen the selection scope of tunable fullerenes for multiple functionalization through their anions in *inter alia* nanocatalysis, organic solar cells and sensor technology. In particular the series of resonances could provide a mechanism for dumping out the hot-carriers thereby eliminating/minimizing their liability in the efficient operation of robust organic solar cells. The HOMO-LUMO energy gaps for the fullerenes are estimated to assess their stability.

INTRODUCTION

In modern organic solar cells the photons absorbed by the donor, usually a polymer create hot-carriers (electrons/holes) which move into the acceptor material, usually a fullerene derivative. Fullerene electron acceptors, commonly employing phenyl-C61-butyric acid methyl ester (PCBM), are widely used in organic solar cells (see [1] and references therein). Associated with the important role played by fullerenes in organic solar cells [2, 3], among their vast applications [4], is understanding of the stability and degradation mechanism of organic solar cells before commercialization can be realized. In [5] the rate of irreversible polymer photobleaching in blend films (polymer:fullerene) was found to consistently and dramatically increase with decreasing electron affinity (EA) of the fullerene derivative. As part of the solution, the authors [5] recommended designing polymers and fullerenes with larger EAs.

Hot (non-equilibrium) carrier thermalization has been identified as one of the major sources of efficiency loss in organic solar cells[6]. The authors proposed an innovative solution, viz. harvesting the hot carriers before they thermalize. This promises to potentially overcome the Shockley-Queisser limit for solar cell efficiency.

Corresponding author:* **Msezane A. Z
Department of Physics and Center for Theoretical Studies of Physical Systems, Clark Atlanta University, Atlanta, Georgia 30314, USA

The importance of the fullerene EAs in catalysis of organic solar cell materials has been investigated and confirmed [5]. The [C_{60}] fullerene hybrids, where the C_{60} is endowed with metal atoms, have demonstrated catalytic efficiency in fundamental hydrogenation [7]. The energy gap E_{gap} between the electronic ground and the first excited states of the neutral fullerene/cluster, viz. HOMO-LUMO energy gap, is an important parameter, determining the stability of a cluster against further chemical reaction [8, 9]. It is used to identify candidates for new cluster materials. A large E_{gap} makes it hard to extract electrons from the low-lying HOMO or add electrons to the high-lying LUMO. The C_{60} and C_{70} gaps were determined to be large [8, 9], with that for C_{60} being 1.61 eV, allowing the authors [8, 9] to conclude that C_{60} is the most stable fullerene. Importantly, the calculated HOMO-LUMO energy gaps for C_{60} and C_{70} [10] differ significantly, by at least a factor of two from those measured in [11, 12].This is a clear demonstration of the difficulty experienced by existing theoretical methods in obtaining reliable data for fullerenes in general and, specifically the challenging electron affinities.

Some suggested techniques to increase fullerene acceptor resistance to degradation by the photo-oxidation mechanism include several options. Namely, 1) the reduction of the

fullerene's LUMO level of the acceptor [1], 2) the employment of fullerenes with high EAs [5], and 3) the use of the highest EA rather than the usual lowest total energy as a predictor of anionic cluster structures because the experimentally detected isomers correspond to the metastable states [13]. These points will become much clearer when we present the results. Indeed, the investigated fullerenes meet all the required characteristics.

Both extensive and intensive investigations are continuing of the role of atomic particles and nanoparticles in catalysis from both fundamental and industrial perspectives. Recently, the novel atomic negative ions have been introduced to the study of atomic and nanoscale catalysis. The interplay between Regge resonances and Ramsauer-Townsend (R-T) minima calculated through complex angular momentum (CAM) analysis has been identified as the fundamental atomic mechanism underlying nanoscale catalysis. Anionic catalysis involves the weakening or breaking up of molecular bonds in the transition state [14].

Also, low-energy electron scattering resonances have been linked directly with chemical reaction dynamics, thereby allowing us to probe sensitively electron attachment in complex atomic systems and fullerenes resulting in short- and long-lived negative ion formation[15, 16]. At the R-T minimum, the electrons traverse through as though the molecules were transparent. Thus, the R-T minimum provides an excellent environment and mechanism for breaking up molecular bonds in new molecules creation as well as in anionic catalysis [14]. The R-T effect has also been exploited to understand sympathetic cooling and to produce cold molecules employing natural fermions [17].

The experiments of Hutchings and collaborators involving the production of hydrogen peroxide (H_2O_2) from H_2O catalyzed by the Au and Pd nanoparticles [18, 19] were explained through the fundamental mechanism of negative ion catalysis[14]. Namely, the Au^- and Pd^-anions formed during the collision process break up or weaken the H-O bonds and in the presence of oxygen, the H_2O_2 formation results[14]. Recently, the same group [20] has developed a method of producing H_2O_2 catalyzed through a Pd-Sn catalyst involving a simple one-step process; note the replacement of Au by the less expensive Sn. This promises to make the production of H_2O_2 readily available to the developing world where it could be used for water purification as well [20].

Since the experiments [18, 19], it has been our fervent desire to discover a single multifunctional anionic catalyst to replace the nanocatalysts in the experiments [18-20]. With the current investigations we believe that we have found an excellent catalyst in the fullerenes as well as the attendant fundamental mechanism of catalysis. For the catalyst to work, we require that its negative ion form at the second R-T minimum of the electron elastic scattering total cross section (TCS) and that the binding energy (BE) of such an anion (or equivalently the EA) be relatively large and approximately equal to the vertical detachment energy (VDE), in this case water. The figures under the results section demonstrate the potential for achieving this and catalyzing many more reactions, including the catalysis of methanol from CH_4 without CO_2 emission [21].

Electron-electron correlations and core-polarization interaction are the major physical effects responsible for electron attachment in low-energy electron scattering from heavy complex atomic systems and fullerenes, leading to stable negative ion formation as resonances. In the Regge-pole methodology the electron-electron correlation effects are fully embedded through the Mullholland formula while the polarization interaction is accounted for by the robust Avdonina-Belov-Felfli (ABF) potential[16]. The first application of the Regge pole methodology to low-energy electron scattering from fullerenes obtained the unprecedented theoretical binding energies (BEs) for the negative ions C_n^-(n=60, 70, 74, 76, 78, 80, 82, 84, 86, 90, 92) that matched excellently the measured EAs [22-31]; this theoretical feat has never been accomplished before.This is the reason why the ground state anionic BE and the EA are interchangeable in this paper. Accurate atomic and molecular EAs are crucial to the understanding of chemical reactions involving anions [32]. The importance and utility of atomic and molecular negative ions in terrestrial and stellar atmospheres as well as in device fabrication have already been reported[4, 33-37]

Low-energy electron scattering cross sections for complex and heavy atoms including fullerenes are characterized generally by R-T minima, shape resonances (SRs) and dramatically sharp resonances manifesting stable negative ion formation [14-16]. In this paper the Regge pole methodology has been used to explore low-energy electron scattering from the fullerenes C_n(n=94, 96, 98, 120, 136) in the electron impact energy range $0.0 \leq E \leq 10.0$ eV to identify and delineate the resonances in the electron elastic TCSs and extract the BEs of the resultant anions formed during the collisions. The main objective is to discover the variation of the resonance structures as the fullerene size varies from C_n(n=94 through 136); viz. determine the size effect on the TCSs (tenability of the resonances through size). We also extract from the TCSs the R-T minima, SRs and the BEs of the resultant negative ions formed during the collisions as resonances. These results are also intended to guide the selection of suitable fullerenes for organic solar cells and other applications. The important HOMO-LUMO energy gaps for the fullerenes are also estimated to guide measurements.

Method of Calculation

For the near-threshold electron-neutral fullerene collisions resulting in negative ion formation as resonances, we calculate TCSs using the Mulholland formula [38]. In the form below, the TCS fully embeds the electron-electron correlation effects [39] (atomic units are used throughout):

$$\sigma_{tot}(E) = 4\pi k^{-2}\int_0^\infty \mathrm{Re}[1-S(\lambda)]\lambda d\lambda$$
$$-8\pi^2 k^{-2}\sum_n \mathrm{Im}\frac{\lambda_n \rho_n}{1+\exp(-2\pi i\lambda_n)} + I(E) \qquad (1)$$

In Eq. (1) S is the S-matrix, $k=\sqrt{2mE}$, with m being the mass and E the impact energy, ρ_n is the residue of the S-matrix at the n^{th} pole, λ_n and $I(E)$ contains the contributions from the integrals along the imaginary λ-axis; its contribution has been demonstrated to be negligible [40].

As in [41] here we consider the incident electron to interact with the fullerene without consideration of the complicated details of the electronic structure of the fullerene itself. Therefore, within the Thomas-Fermi theory, Felfli *et al* [42] generated the robust potential

$$U(r) = -\frac{Z}{r(1+\alpha Z^{1/3} r)(1+\beta Z^{2/3} r^2)} \quad (2)$$

Where Z is the nuclear charge, α and β are variation parameters. Notably, our choice of the potential, Eq. (2), is adequate as long as we limit our investigation to the near-threshold energy regime, where the elastic cross section is less sensitive to short-range interactions and is determined mostly by the polarization tail. Note also that the potential (2) has the appropriate asymptotic behavior, *viz.* $U(r) \sim -1/(\alpha\beta r^4)$ and accounts properly for the crucial polarization interaction at low energies. The advantage of the well-investigated [43-45] potential (2) is that it is a good analytic function that can be continued into the complex plane. The effective potential $V(r) = U(r) + \lambda(\lambda+1)/2r^2$ is considered here as a continuous function of the variables r and complex λ.

The potential (2) has been used successfully with the appropriate values of α and β. It has been found that when the TCS as a function of β has a resonance [40], corresponding to the formation of a stable bound negative ion, this resonance is longest lived for a given value of the energy, which corresponds to the EA of the system (for ground state collisions) or the BE of the excited anion. This was found to be the case for all the systems, including fullerenes we have investigated thus far. This fixes the optimal value "β" in Eq. (2) when the optimum value of $\alpha = 0.2$. The use in this paper of different values of the optimal parameter "β" for the ground and excited fullerenes is supported by the study of low-energy electron scattering from Cu atoms [46]. There it was demonstrated that the ground and excited states are polarized differently as expected, namely both the dipole polarizability and quadrupole polarizability for the ground and the excited atomic Cu were found to be different.

The details of the numerical evaluations of the TCSs have been described in [39] and further details of the calculations may be found in [47]. In the Regge pole description of low-energy electron scattering from complex atomic, molecular and cluster systems leading to negative ion formation as resonances, Regge trajectories, viz. $\mathrm{Im}\,\lambda(\mathrm{E})$ versus $\mathrm{Re}\,\lambda(\mathrm{E})$ are the crucial calculated quantities; the explicit dependence on E of λ is inserted for clarity. The Regge trajectories penetrate the atomic/molecular/cluster core and for the methodology to work very well, it is required that we stay close to the real axis of the complex angular momentum. This implies that $\mathrm{Im}\,\lambda$ (E) should remain small within the electron impact energy of interest.

For a better understanding and appreciation of the use of the Regge trajectories, here we explain the effective use of the pole λ (complex angular momentum) in the Mulholland formula, Eq.(1). From the pole λ, where $\mathrm{Re}\,\lambda(\mathrm{E})$ is an integer and $\mathrm{Im}\lambda(\mathrm{E})$ $(=\lambda_I) \rightarrow 0$, we can determine from Eq. (1) the shape resonances, long-lived metastable anions and ground state anionic resonances. The effective use of $\mathrm{Im}\lambda(\mathrm{E})$, $\lambda_I \rightarrow 0$ is demonstrated in the paper [40]. Although we have previously referred to Connor [48] for the physical interpretation of $\mathrm{Im}\,\lambda(\mathrm{E})$, the original interpretation was given by Regge himself [49]. The resonance width in energy is Γ while λ_I represents its width in angular momentum. The conjugate variable to energy is time, and the lifetime Δt of the resonance satisfies the relation $\Delta t = 1/\Gamma$. Similarly, the conjugate variable in angular momentum is angle, and the angle $\Delta\theta$ through which the particle orbits during the course of the resonance satisfies the relation $\Delta\theta = 1/\lambda_I$. For a long-lived resonance, the lifetime λ_I is small and $\Delta\theta$ is large. For a true bound state, $\mathrm{Im}\,\lambda(\mathrm{E})$ vanishes and the orbit becomes permanent. Obviously, in our calculations $\mathrm{Im}\,\lambda(\mathrm{E})$ is not identically zero, but small – this can be clearly seen in the figures: the long-lived resonances hardly have a width as opposed to shape resonances for instance (see also [40] for comparison). This means that technically the corresponding state is not a true bound state. This is acceptable, since most negative ions do not have an infinite lifetime, i.e. they eventually decay.

RESULTS

Here we first describe a general characteristic behavior of all the TCSs presented in the Figs. 1-5 using the results of Fig. 1. In Fig. 1 there are two prominent groups of the dramatically sharp resonances. The first is bounded by the ground state resonance located at the deepest R-T minimum representing the ground state of the formed negative ion with the BE of 3.27 eV, which has previously been identified with the measured EAs in other fullerenes [16]. The second group belongs to the excited states, the brown and the green curves. Most important here is that the green curve characterizes the atomic behavior consistent with the view that fullerenes behave like "big atoms" [50]. This limiting green curve is robust and has been traced back through C_{60} to C_{44} to C_{28} and eventually to C_{20}, the smallest fullerene thought to exist. Indeed, it is the same curve that appears as an excited state in the TCS of atomic Au. As demonstrated in [16] the ground state curve is similar to that of atomic Au as well. The main difference is that the fullerene TCSs are charactetrized generally by a SR near threshold while the atomic TCSs begin with a decreasing slope. Suffice to state that the fullerene size effect introduces through the polarization interaction more metastable resonances and excited states resonances - these are associated with the green curve in Fig. 1. Contrary to the fullerene case, in the atomic case the first R-T minimum of the green curve is much lower than the second R-T minimum and the sharp resonance is not at the absolute minimum. The long-lived metastable curves are associated with the anionic ground state resonance. Clearly, the ground state and the excited state resonances provide rigid confining boundaries for the fullerene TCSs and the size impacts the TCSs inbetween.

The TCSs presented in each of the Figs 1-5 appear to be complicated. However, these figures are easily understood and interpreted if we focus on a single color-coded curve at a time determined by an appropriately optimized value of the β parameter (polarization interaction). The various color-coded curves in each figure represent scattering from different states of the same fullerene resulting in negative ion formation; a ground state, metastable states and higher excited states. They result from the fact that the electron attaches itself to the fullerene in different states (ground, metastable and higher excited states) and the difference between these curves is determined essentially by the polarization potential. The subtle differences among the various figures, fullerene specific and curves make these fullerenes especially important in many chemical reactions applications.

Figure 1 contrasts the ground state TCS (red curve) with the polarization induced metastable state TCSs (blue and pink curves) for the e - C_{94} scattering; the brown and green curves represent the TCSs for excited states. All the TCSs in the figure are characterized by R-T minima, SRs and dramatically sharp resonances corresponding to the C_{94}^- fullerene negative ions formation. The BE of the ground state of the C_{94}^- anion is located at the absolute R-T minimum of the TCS and as was found previously for other fullerenes [16, 22-31] determines the EA of C_{94}. We now focus on the ground state curve, red curve. It is characterized by two SRs (one near the threshold at about 0.075 eV and the other is at about 1.20 eV) and two R-T minima. The first R-T minimum just before the second SR is shallow while the other is deep, within which appears the dramatically sharp resonance at 3.27 eV, representing the formed stable ground state of the C_{94}^- anion.

The physics is as follows. As the electron approaches closer, the fullerene becomes polarized, reaching maximum polarization manifested by the appearance of the first R-T minimum at about 0.90 eV. With the increase in energy, the electron becomes trapped by the centrifugal potential, whose effect is seen through the appearance of the SR at about 1.2 eV. As the electron leaves the C_{94} fullerene, the strong polarizability of the C_{94} shell leads to the creation of the deep R-T minimum at whose absolute minimum the long-lived ground state C_{94}^- anion is formed; its BE is seen to be 3.27 eV. At the R-T minimum the C_{94} is transparent to the incident electron and the electron becomes attached to it forming the stable C_{94}^- anion. The electron spends many angular rotations about the C_{94} as it decays. The long angular life time is determined by $1/\mathrm{Im}\,\lambda \to \infty$, since $\mathrm{Im}\,\lambda \to 0$, see Eq. (1). Indeed, the results demonstrate the crucial importance of the polarization interaction. They are consistent with the conclusion in [51] that the appearance of the R-T minima in the electron scattering cross sections manifest that the polarization interaction has been accounted for adequately in the calculation.

Next, we consider the long-lived polarization induced metastable TCSs for C_{94}, represented by the blue and pink curves. Each TCS like that of the ground state is also characterized by two SRs and two R-T minima. Importantly, the BEs of each of the polarization induced long-lived metastable anions are significant, viz. 2.30 eV and 1.36 eV; they also appear at their respective absolute R-T minima of the TCSs. The BEs of the excited anionic states of the C_{94} are 0.408 eV and 0.326 eV. The two metastable TCSs with anionic BEs of 2.30 eV and 1.36 eV are of particular importance and interest here. Since we are also searching for nanocatalysts through their anions, we observe that the BE of 2.30 eV of the long-lived metastable resonance is very close to the measured EA of Au [52, 53]. Consequently, the C_{94} could be used to replace the Au, Pd and Sn catalysts in the experiments of Hutchings and collaborators [18-20]. Also, the results of Fig.1 provide part of the requirement to increase fullerene acceptor resistance to degradation by the photo-oxidation mechanism, viz. employment of fullerenes with high EAs and the use of the highest EA rather than the usual lowest total energy as a predictor of anionic cluster structures [13]. These results could also provide a mechanism for dumping the hot carriers through the series of resonances of Fig. 1. Indeed, the TCSs in Fig. 1 also confirm directly the experimental observation that low energy (0-15 eV) electron-fullerene interactions are characterized by very long-lived metastable anions formation [54-57].

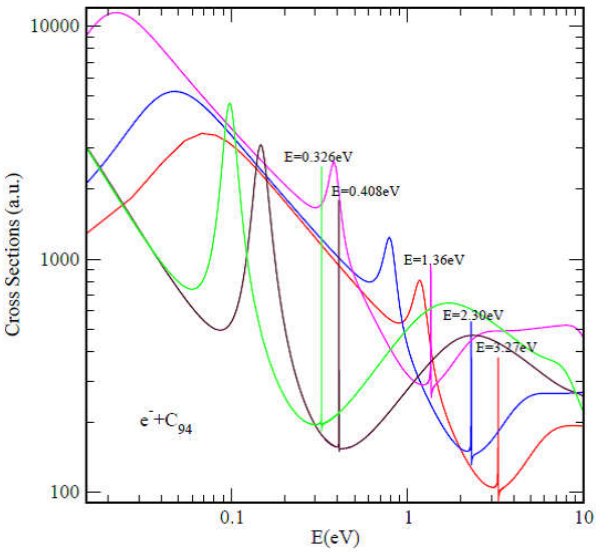

Figure 1 Total cross sections (a.u.) for electron elastic scattering from C_{94}. The red, blue and pink curves represent results for the ground and metastable (first and second), respectively; the brown and green curves represent the TCSs for the first and second excited states, respectively. The dramatically sharp resonances correspond to the C_{94}^- anionic formation during the collisions.

In Figure 2 we present the e – C_{96} scattering TCSs. Except for the subtle differences in the details of the BEs of the anions, important in catalysis, sensor technology and organic solar cells, overall the TCSs resemble those of Fig. 1.

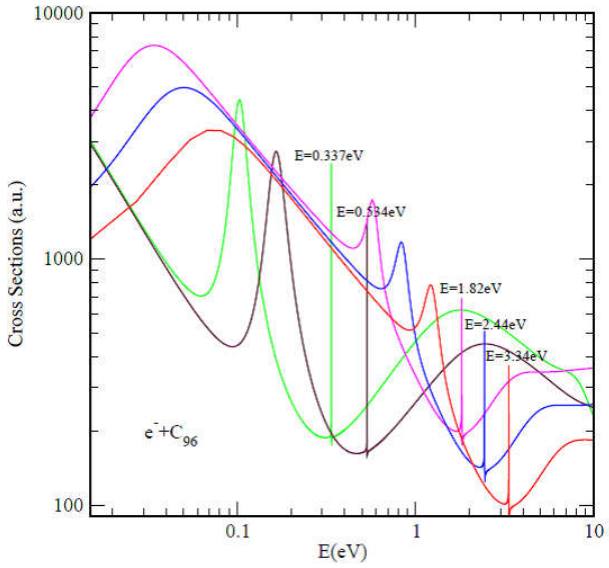

Figure 2 Total cross sections (a.u.) for electron elastic scattering from C_{96}. The red, blue and pink curves represent results for the ground and metastable (first and second), respectively; the brown and green curves represent the TCSs for the first and second excited states, respectively. The dramatically sharp resonances correspond to the C_{96}^- anionic formation during the collisions.

The description and the relevant physics are similar. The significant size effect is evident in the 1.36 eV metastable and the 0.408 eV excited states resonances of C_{94}. In C_{96} these values have increased to 1.82 eV and 0.534 eV, respectively. Essentially, the energy positions of these resonances are impacted the most by the size effect and we will follow them as the fullerene size evolves from C_{96} through C_{136}. Additionally, sensitive to the change from C_{94} to C_{96} is the

metastable TCS (pink curve) manifested through its shape resonances. In C_{94} the near threshold SR with BE of 0.023 eV has TCS magnitude of about 11,500. a.u. while the second SR has BE of 0.40 eV and TCS magnitude of approximately 2,700. a.u. In C_{96} the same curve has values of 0.034 eV, 7,300. a.u. and 0.60 eV, 1,700. a.u. respectively. Clearly, the change from C_{94} to C_{96} impacts the relevant TCSs and the attendant SRs significantly.

Figure 3 presents the TCSs for e – C_{98} scattering. These TCSs are essentially similar to those of C_{96}. However, the ground state BE of the C_{98}^- anion is larger than those of the C_{94}^- and C_{96}^- anions. In fact, it is among the largest BEs found among the five investigated fullerenes in this paper. Also, the BE of the first excited state of the C_{98}^- anion is smaller than that of the C_{96}^- anion. Indeed, the C_{98} could be used to catalyze through its anions H_2O_2 from H_2O at 2.48 eV and 1.90 eV, thereby possibly replace the Au and Pd as well as the Sn catalysts in the experiments of Hutchings and collaborators [18-20]. Additionally, it could provide the needed fullerene for organic solar cells [5] because of its large anionic ground state BE (EA).

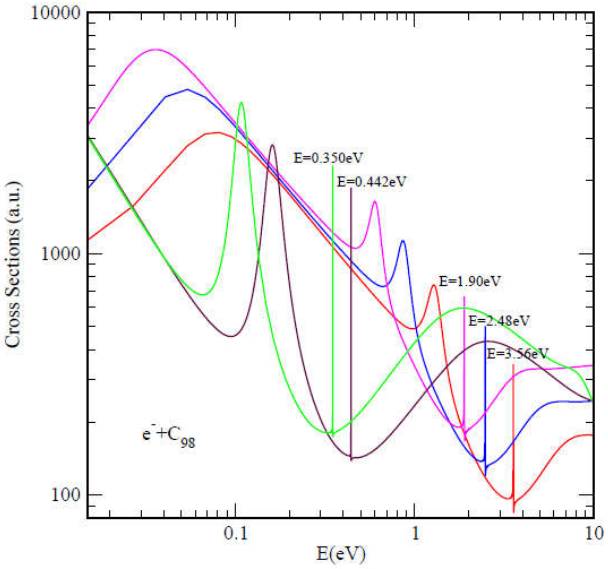

Figure 3 Total cross sections (a.u.) for electron elastic scattering from C_{98}. The red, blue and pink curves represent results for the ground and metastable (first and second), respectively; the brown and green curves represent the TCSs for the first and second excited states, respectively. The dramatically sharp resonances correspond to the C_{98}^- anionic formation during the collisions.

Figure 4 contrasts the TCSs for e – C_{120} scattering; they are also characterized by SRs, R-T minima and dramatically sharp resonances located at their second R-T minima, representing C_{120}^- anionic formation. The TCSs behavior is essentially similar to that of the C_{98} fullerene. However, the change from C_{98} to C_{120} affects significantly the resonance structures and the BEs for the ground state and the two metastable states of C_{98}^- through the introduction of a ground state anion with BE of 3.74 eV, located at the second R-T minimum.

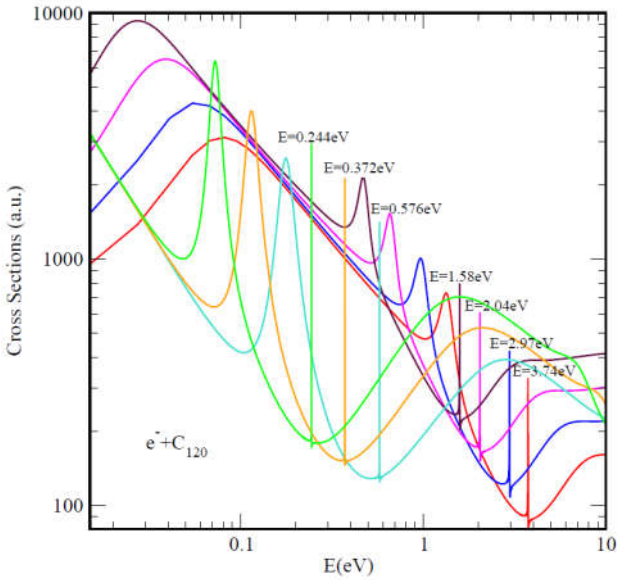

Figure 4 Total cross sections (a.u.) for electron elastic scattering from C_{120}. The red, blue, pink and brown curves represent results for the ground and metastable (first, second and third), respectively; the light blue, orange and green curves represent the TCSs for the first, second and third excited states, respectively. The dramatically sharp resonances correspond to the C_{120}^- anionic formation during the collisions.

It is noted that there are three metastable and a ground states anions in the TCSs for C_{120} as well as three excited anionic states. This is the largest number found thus far in any fullerene investigated. These marching resonances could then be used to dump the hot carriers thereby eliminate their liability to organic solar cells efficient utilization. The impact of the size on the TCSs is evident as the fullerene changes from C_{98} to C_{120}.

Notably, the ground state and the first metastable state BEs of the formed anions in the electron scattering TCSs of C_{120} are the largest of the investigated C_{94}, C_{96} and C_{98} fullerenes. The BEs of the two excited states of C_{98}^-, namely 0.350 eV and 0.442 eV are barely influenced by the transition from C_{98} to C_{120}. Importantly, the significant size effect is manifested through the introduction of the additional metastable state anion with the BE of 1.58 eV and the excited state anion with the BE of 0.576 eV in the TCSs of C_{120} compared to those of the C_{94}, C_{96} and C_{98}. These results are a clear demonstration that the response of each fullerene to gentle electron impact should be carefully examined. Because of the sensitivity of some of the results to the fullerene size effects, these results could be useful in sensor technology and catalysis of various processes, including methane oxidation without CO_2 emission [21]. Since the C_{120}^- ground state anion has a large BE, it should satisfy one of the requirements for fullerene accept or resistance to degradation by the photo-oxidation mechanism. From the examination of the behavior of the two sets of resonances (those associated with the ground state and those with the excited states) in the C_{120} TCSs it appears that they will eventually merge as the fullerene size increases; this warrants further investigations.

In Figure 5 is plotted the TCSs for the e - C_{136} scattering. Here we observe the significant impact of the size effect provided by the C_{136} fullerene compared to C_{94}, C_{96} and C_{98} as well as to C_{120}. Although the BEs of the anionic ground states of the C_{120} and C_{136} fullerenes are essentially the same, the BEs of the three metastable states associated with the ground states differ significantly, manifesting the strong size-dependence of the anionic formation in the two fullerenes.

Particularly interesting in the TCSs for C_{136} is that all the formed metastable negative ionic resonances, namely those at 2.64 eV, 2.19 eV and 1.67 eV are members of the ground state TCS curve. On the

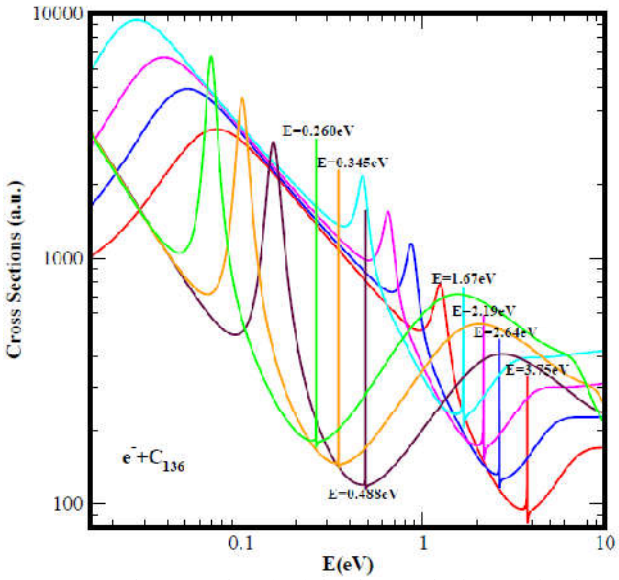

Figure 5 Total cross sections (a.u.) for electron elastic scattering from C_{136}. The red, blue, pink and light blue curves represent results for the ground and metastable (first, second and third), respectively; the brown, orange and green curves represent the TCSs for the first, second and third excited states, respectively. The dramatically sharp resonances correspond to the C_{136}^- anionic formation during the collisions

other hand, in the TCSs for C_{120} only the anionic resonances with BEs of 2.97 eV and 2.04 eV belong to the ground state curve; the anionic resonance at 1.58 eV is a member of the second metastable curve. These results clearly demonstrate the intricate size-dependence of the resonance structures. Except for the first excited anionic state whose BE is 0.488 eV, the set of the excited anionic resonances appear less sensitive to the fullerene size. These results demonstrate that the C_{136} fullerene like the C_{120} can be operated at a wider energy spectrum as a chemical sensor and a nanocatalyst through its negative ions; it also provides a larger BE through its ground state anion. Indeed, these fullerenes C_{136} and C_{120} because of their large EAs (ground state anionic BEs) compared to the C_{60} EA of 2.683 eV [24], are capable of accepting multiple electrons in the condensed phase. The large ground state anionic BE of 3.75 eV for the C_{136}qualifies it for use in organic solar cells [5]. Additionally, the series of resonances could be useful in dumping the hot carries, thereby eliminating or minimizing their liability in the operation of a robust organic solar cell. It is further noted that the three metastable resonances are within the R-T minimum of the ground state TCS of C_{136}; therefore, the C_{136} could be used for multiple catalysis as well. The important results of the Figs. 1-5 are summarized and contrasted in Table 1. Notably, the ground state BEs for these fullerenes are consistent with those calculated in [16] and the measured EAs in [22-31]. The calculated TCSs and the extracted BEs of the formed negative ions during the electron-fullerene collisions should help in the construction of the popular model potential wells for those fullerenes and the corresponding endohedral fullerenes through their negative ions BEs [58-62]. Importantly, the data in Figs. 1 through 5 and in Table 1 allow us to estimate the HOMO-LUMO energy gaps for the fullerenes studied as was done in [27]. For the C_{94}, C_{96}, C_{98}, C_{120} and C_{136} fullerenes we use the BEs in the column MS-2 of Table 1. For all the excited states we use the corresponding values in the column EXT-1.

The determined HOMO-LUMO energy gaps for C_{94}, C_{96}, C_{98}, C_{120} and C_{136} are 1.05 eV, 1.29 eV, 1.46 eV, 1.46 eV and 1.18 eV, respectively. As expected, all these fullerenes have HOMO-LUMO energy gaps smaller than those for the stable C_{60} and C_{70} fullerenes [27]; therefore they are less stable than the C_{60} and C_{70}fullerenes. However, among the investigated fullerenes it can be concluded that C_{120} and C_{98} are the more stable ones; this requires experimental verification and facilitates further experimental exploration of the larger fullerenes. It is noted that to our knowledge the TCSs for the investigated fullerenes are the first and only. The attendant anionic binding energies, Ramsauer-Townsend minima and shape resonances are also the first as well as the electron affinities of these large fullerenes. Since the investigated fullerenes possess large EAs; they are capable of accepting multiple electrons in the condensed phase.

CONCLUSION

The rich long-lived metastable resonances that characterize the Regge pole calculated fullerenes TCSs presented for the first time in this paper support the important conclusion that the experimentally detected fullerene isomers correspond to the metastable states [13]. And further confirm the need to identify and delineate the resonance structures in gentle electron scattering, since the formed anions determine the fullerene nanocatalysis mechanism. Also we found relatively large ground state BEs for resultant anions, as high as 3.56 eV for the C_{98}^-, 3.74 eV for the $C_{120}^-$and 3.75 eV for the C_{136}^-anions (equivalent to the EAs for these fullerenes). These should satisfy part of the requirement to increase fullerene acceptor resistance to degradation by the photo-oxidation mechanism through the employment of fullerenes with high EAs [5] and guide both experimental and theoretical exploration of these large fullerenes. Importantly, a single large fullerene such as the C_{136} or even the C_{96} could replace the Au, Pd and Sn atoms in the catalysis of H_2O_2 from H_2O in the experiments of Hutchings and collaborators [18-20] acting as a ultiple functionalized nanocatalyst. This could certainly reduce the cost further and provide dynamic H_2O_2 nanocatalysis for water purification in the developing world [20]. It is noted that many more reactions could be catalyzed with the appropriate vertical detachment energy matching the anionic BEs in the figures. These fullerenes could also be combined to form supper multiple catalysts/sensors for various chemical reactions as well as used as multiple electron acceptors in the condensed phase.

Finally, these results are expected to impact new materials design and creation significantly through the fundamental understanding of gentle electron processes at the atomic and nano scales. And the robust Regge pole methodology, representing an unprecedented theoretical breakthrough in low-energy electron-cluster collision will certainly continue to be used to identify suitable fullerenes for various applications, including in organic solar cells and nanocatalysis. To our knowledge the TCSs for the fullerenes presented in this paper are the first and only. The corresponding anionic BEs, R-T minima, SRs are also the first as well as the important EAs of the investigated fullerenes C_{94}, C_{96}, C_{98}, C_{120} and C_{136}.

Acknowledgments

This research was supported by the US DOE, Division of Chemical Sciences, Geosciences and Biosciences, Office of Basic Energy Sciences, Office of Energy Research. The computing facilities of the National Energy Research Scientific Computing Center are greatly appreciated.

Table 1 Negative ion binding energies (BEs), in eV and energy positions of Ramsauer-Townsend (R-T) minima, in eV obtained from the TCSs for the fullerenes C_{94}, C_{96}, C_{98}, C_{120} and C_{136}. GR-S, MS-*n* and EXT-*n*(*n*= 1, 2, 3) represent respectively ground, metastable and excited states.

System	BEs (eV) GR-S	BEs (eV) MS-1	BEs (eV) MS-2	BEs (eV) MS-3	BEs (eV) EXT-1	BEs (eV) EXT-2	BEs (eV) EXT-3	R-T (eV) GR-S	R-T (eV) MS-1	R-T (eV) MS-2	R-T (eV) MS-3
C_{94}	3.27	2.30	1.36	-	0.408	0.326	-	3.05	2.17	1.22	-
C_{96}	3.34	2.44	1.82	-	0.534	0.337	-	3.15	2.30	1.70	-
C_{98}	3.56	2.48	1.90	-	0.442	0.350	-	3.33	2.36	1.77	-
C_{120}	3.74	2.97	2.04	1.58	0.576	0.372	0.244	3.57	2.81	1.93	1.60
C_{136}	3.75	2.64	2.19	1.67	0.488	0.345	0.260	3.51	2.60	2.01	1.53

References

1. E. M. Speller, *Materials Science and Technology* 33 (8), 924 (2017)
2. V. K. Voorat, L. S. Cederbaum, K. D. Jordan, *J. Phys. Chem. Lett.* 4 (6), 848 (2013); *J. N. Bull, J*. R. R. Verlet, Science Advances 3 (5), 1603106 (2017); B. C. Thomson, J. M. J. Frechet, Angew Chem. Int. Ed. 47, 58 (2008); Y. Kim, S. Cook, S. M. Tuladhar, S. A. Choulis, J. Nelson, J. R. Durrant, D. D. C. Bradley, M. Giles, I. Mcculloch, C. S. Ha, M. Ree, *Nature Materials* 5, 197 (2006).
3. A. V. Nenashev, M. Wiemer, A. V. Dvurechenski, L.V. Kulik, A. B. Pevtsov, F. Gebhard, M. Koch, S. D. Baranovskii, *Phys. Rev*. B 95, 104207 (2017); I. Constantinou, X. Yi, N. T. Shewmon, E. D. Klump, C. Peng, S. Garakyaraghi, C. K. Lo, J. R. Reynolds, F. N. Castellano, F. So, Adv. *Energy Mat.* 7 (13), 1601947 (2017).
4. M. S. Dresselhaus, G. Dresselhaus, P. C. Eklund, Science of Fullerenes and Carbon Nanotubes, Academic Press, Boston, MA 1996
5. E. T. Hoke, I. T. Sachs-Quintana, M. T. Lloyd, I. Kauvar, W. R. Mateker, A. M. Nardes, C. H. Peters, N. Kopidakis, M. D. McGehee, *Adv. Energy Mat*. 2, 1351 (2012)
6. Z. Guo, Y. Wan, M. Yang, J. Snaider, K. Zhu, L. Huang, *Science* 356, 59 (2017)
7. S. Vital, J. Marco-Martinez, S. Filippone and N. Martin, *Chem. Commun*. 53, 4842 (2017)
8. B. L. Zhang, C. H. Xu, C. Z. Wang, C. T. Chan, K. M. Ho, *Phys. Rev*. B 46, 7333 (1992)
9. H. Kietzmann, R. Rochow, G. Ganteför, W. Eberhardt, K. Vietze, G. Seifert, P. W. Fowler, *Phys. Rev. Lett*. 81, 5378 (1998)
10. N. Shao, Y. Gao, C. Zeng, *J. Phys. Chem*. C 111, 17671 (2007)
11. S. H. Yang, C. L. Pettiette, J. Conceicao, O. Cheshnovsky, R. E. Smalley, *Chem. Phys. Lett*. 139, 233 (1987)
12. P. W. Fowler and D.E. Manolopoulos, An Atlas of Fullerenes, Clarendon Press, Oxford, 1995
13. L. Kronik, R. Fromherz, E. Ko, G. Ganteför and J. R. Chelikowsky, *Nature Materials* 1, 49 (2002)
14. A. Z. Msezane, Z. Felfli, D. Sokolovski *J. Phys. B* 43, 201001 (2010) (FAST TRACK)
15. Z. Felfli, A.Z. Msezane, D. Sokolovski, *J. Phys. B* 45, 045201 (2012)
16. Z. Felfli, A. Z. Msezane, *Euro Phys. J.* D, At Press (2017)
17. S. Aubin, S. Myrskog, M. H. T. Extavour, L. J. LeBlanc, D. McKay, A. Stummer, J. H. Thywissen, *Nat. Phys*. 2, 384 (2006)
18. J. K. Edwards, A. F. Carley, A. A. Herzing, C. J. Kiely, G. J. Hutchings, *J. Chem. Soc*., Faraday Discuss. 138, 225 (2008)
19. J. K. Edwards, B. Solsona, P. Landon, A. F. Carley, A. Herzing, M. Watanabe, C. J. Kiely, G. J. Hutchings, *J. Mater Chem*. 15, 4595 (2005)
20. S. J. Freakley, Q. He, J. H. Harrhy, L. Lu, D. A. Crole, D. J. Morgan, E. N. Ntainjua, J. K. Edwards, A. F. Carley, A. Y. Borisevich, C. J. Kiely, G. J. Hutchings, *Science* 351, 959 (2016)
21. A. Z. Msezane, Z. Felfli, A. Tesfamichael, K. Suggs, X.Q. Wang, Gold Bulletin 45, 127 (2012)
22. L.-S. Wang, J. J. Conceicao, C. M. Jin, R. E. Smalley, *Chem. Phys. Lett*. 182, 5 (1991)
23. C. Brink, L. H. Andersen, P. Hvelplund, D. Mathur, J. D. Voldstad, *Chem. Phys. Lett*. 233, 52 (1995)
24. D. -L. Huang, P. D. Dau, H. -T. Liu, L. -S. Wang , *J. Chem. Phys*. 140, 224315 (2014)
25. 25] O. V. Boltalina, L. N. Sidorov, E. V. Sukhanova, E. V. Skokan, Rapid Commun. *Mass Spectrom*.7, 1009 (1993)
26. X. -B. Wang, C. -F. Ding, L. -S. Wang, *J. Chem. Phys*. 110, 8217 (1999)
27. X. B. Wang, H. -K. Woo, J. Yang, M. M. Kappes, L. S. Wang, *J. Phys. Chem*. C 111, 17684 (2007)
28. O. V. Boltalina, E. V. Dashkova, L. N. Sidorov, *Chem. Phys. Lett.*256, 253 (1996)
29. O. V. Boltalina, I. N. Ioffe, I. D. Sorokin, L. N. Sidorov, *J. Phys. Chem*. A101, 9561 (1997)
30. X. B. Wang, H. K. Woo, X. Huang, M. M. Kappes, L. S. Wang, *Phys. Rev. Lett*.96, 143002 (2006)
31. X. B. Wang, H. K. Woo, L. S. Wang, *J. Chem. Phys*.123, 051106 (2005)
32. K. Kasdan, W. C. Lineberger, *Phys. Rev. A* 10, 1658 (1974)
33. D. R. Bates, *Adv. At. Mol. Opt. Phys*. 27, 1 (1991)
34. C. Blondel, *Phys. Scr*. T 58, 31 (1995)
35. T. Andersen, *Phys. Rep*. 394, 157 (2004)
36. D. J. Pegg, Rep. *Prog. Phys*.67, 857 (2004)
37. S. T. Buckman, C. W. Clark, Rev. Mod. Phys. 66, 539 (1994)
38. H. P. Mulholland, *Proc. Camb. Phil. Soc*. (London) 24, 280 (1998)
39. D. Sokolovski, Z. Felfli, S. Yu. Ovchinnikov, J. H. Macek, A. Z. Msezane, *Phys. Rev. A* 76, 026707 (2007).
40. Z. Felfli, A. Z. Msezane, D. Sokolovski, *Phys. Rev. A* 79, 012714 (2009).
41. V. K. Dolmatov, M. Ya.Amusia, L.V. Chernysheva, *Phys. Rev. A* 95, 012709 (2017)
42. Z. Felfli, S. Belov, N. B. Avdonina, M. Marletta, A. Z. Msezane, S. N. Naboko, in Proceedings of the Third International Workshop on Contemporary Problems in Mathematical Physics (Eds: J. Govaerts, M. N. Hounkonnou, A. Z. Msezane), World Scientific, Singapore 2004, pp. 218-232
43. S. M. Belov, N. B. Avdonina, Z. Felfli, M. Marletta, A. Z. Msezane, S. N. Naboko*, J. Phys*. A 37, 6943 (2004).
44. K. -E. Thylwe, P. McCabe, *Eur. Phys. J*. D 68, 323 (2014).
45. S. Belov, K. -E. Thylwe, M. Marletta, A. Z. Msezane, S. N. Naboko*, J. Phys A* 43, 365301 (2010).
46. S. Y. Yousif Al-Mulla, *Eur. Phys. J*. D42, 11 (2007).
47. P. G. Burke, C. Tate, Comp. *Phys. Commun*. 1, 97 (1969).
48. J. N. L. Connor, *J. Chem. Soc. Faraday Trans*.86, 1627 (1990).
49. T. Regge, NuovoCimento18, 947 (1960)
50. M. Ya. Amusia, *Chem. Phys*. 414, 168 (2013)
51. W.R. Johnson, C. Guet, *Phys. Rev*. A 49, 1041 (1994).
52. H. Hotop, W. C. Lineberger, *J. Phys. Chem. Ref. Data* 14, 731 (1985); T. Andersen, H. K. Haugen, H. Hotop*, J. Phys. Chem. Ref. Data* 28 (6), 1511 (1999)
53. W. Zheng, X. Li, S. Eustis, A. Grubisic, O. Thomas, H. De Clercq, K. Bowen K, *Chem. Phys. Le*tt. 444, 232 (2007)
54. O. Elhamidi, J. Pommier, R. Abouaf, *J. Phys. B: Atom. Mol. Phys.* 30, 4633 (1997)
55. M. Lezius, P. Scheier, T. D. Märk, *Chem. Phys. Lett*. 203, 232 (1993)
56. T. Jaffke, E. Illenberger, M. Lezius, S. Matejcik, D. Smith, T. D. Märk, *Chem. Phys. Lett*. 226, 213 (1994)
57. J. Huang, H. S. Carman, R. N. Compton, *J. Phys. Chem*. 99, 1719 (1995)
58. M. J. Pushka, R. M. Nieminen, *Phys. Rev*. A47, 1181 (1993)
59. M. Ya. Amusia, A. S. Baltenkov, B. G. Krakov, *Phys. Lett*. A 243, 99 (1998)
60. A. S. Baltenkov, *Phys. Lett.* A254, 203 (1999)
61. J. P. Connerade, V. K. Dolmatov, P. A. Lakshmi, S. T. Manson, J. Phys. B: At. *Mol. Opt. Phys*.32, L239 (1999)
62. V. K. Dolmatov, A. S. Baltenkov, J. P. Connerade, S. T. Manson, *Rad. Phys. Chem*. 70, 417 (2004)

****